Journal Pre-proofs

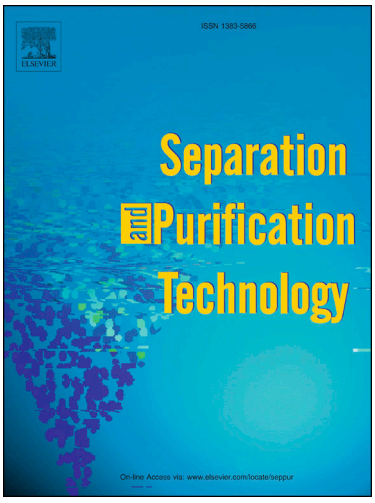

Reversed phase chromatographic separation and downstream precipitation of lupane- and oleanane-type triterpenoids: experiments and modeling based on the method of moments

Ivo S. Azenha, José P.S. Aniceto, Diogo P. Ribeiro, Adélio Mendes, Carlos M. Silva

PII: S1383-5866(20)32681-2
DOI: https://doi.org/10.1016/j.seppur.2020.118208
Reference: SEPPUR 118208

To appear in: *Separation and Purification Technology*

Received Date: 11 August 2020
Revised Date: 8 December 2020
Accepted Date: 10 December 2020

Please cite this article as: I.S. Azenha, J.P.S. Aniceto, D.P. Ribeiro, A. Mendes, C.M. Silva, Reversed phase chromatographic separation and downstream precipitation of lupane- and oleanane-type triterpenoids: experiments and modeling based on the method of moments, *Separation and Purification Technology* (2020), doi: https://doi.org/10.1016/j.seppur.2020.118208

Reversed phase chromatographic separation and downstream precipitation of lupane- and oleanane-type triterpenoids: experiments and modeling based on the method of moments

Ivo S. Azenha[1], José P.S. Aniceto[1], Diogo P. Ribeiro[1], Adélio Mendes[2], Carlos M. Silva[1,*]

[1] CICECO, Department of Chemistry, University of Aveiro, 3810-193 Aveiro, Portugal

[2] LEPABE-Faculdade de Engenharia, Universidade do Porto, 4200-465 Porto, Portugal

*carlos.manuel@ua.pt

Keywords: betulinic acid; oleanolic acid; triterpenoids; triacontyl (C30); simulated moving bed chromatography.

Abstract

The reversed phase chromatographic separation of two triterpenic acids (TTAs), betulinic and oleanolic acids, using a triacontyl (C30) stationary phase was addressed in this work. Methanol, water, acetonitrile, ethanol, isopropanol, ethyl acetate, acetone and mixtures thereof were tested, and the best mobile phase to conduct the separation was found to be methanol/acetonitrile 50/50 (%, v/v) at 23 ^{o}C, taking into account parameters like selectivity, resolution and TTAs solubility. The method of moments was used to determine the equilibrium constants of isotherms, the axial dispersion coefficients and the global linear driving force coefficients of pure betulinic and pure oleanolic acids. These parameters were then successfully validated by modeling unary and binary breakthrough curves. Simulated moving bed calculations showed that betulinic and oleanolic acids can be both obtained with purity of 99.2 % and productivity of 56.2 kg/($m^3_{adsorbent}$ day) using the packing material of an Acclaim C30 column with a 1-1-1-1 configuration with columns of 7.5 cm long. Finally, in order to recover the two TTAs from the SMB extract and raffinate streams, water was envisioned as a precipitation agent. Accordingly, the solubility of each TTA was measured in methanol/acetonitrile 70/30, 50/50, and 30/70 (%, v/v) modified with water. The obtained results showed that adding 65 % (%, v/v) of water it is possible to precipitate 98 % of the dissolved TTAs in all the tested methanol/acetonitrile mixtures.

1. Introduction

An effective and efficient use of biomass industrial residues is through the implementation of integrated biorefineries [1], in which new streams of high value compounds may be generated from what is oftentimes regarded as unavoidable and low value waste [2,3]. Triterpenoids, and markedly triterpenic acids (TTAs), are an example of such high value compounds that can be extracted and isolated from residues of multiple agro-food and agro-forest industries [4], adding significant economic value to biorefinery-based processes.

Betulinic acid (3β-hydroxy-lup-20-en-28-oic acid, BA) and oleanolic acid (3β-hydroxyolean-12-en-28-oic acid, OA) are secondary metabolites produced in plants for protective action and due to their diverse nutraceutical and pharmacological properties (e.g., antidiabetic, antioxidative, anti-inflammatory, anti-viral and anti-tumoral properties [5,6]) have attracted considerable research interest in the last few years. Betulinic acid has been extensively studied in the literature as having the ability to inhibit HIV (human immunodeficiency virus) [7] and one of the pharmacological properties attributed to oleanolic acid is its hepatoprotective effect [8]. These naturally occurring isomeric triterpenic acids ($C_{30}H_{48}O_3$) possess lupane (BA) and oleanane (OA) carbon backbones and are ubiquitously distributed in numerous plants and edible fruits, being consequently integrated in human diet [9]. Oleanolic acid, for instance, can be isolated from over 1600 plant species [10], and its daily intake (*per* capita) in Mediterranean countries is estimated to be between 17 and 25 mg [11].

Due to their broad spectrum of pharmacological properties, these TTAs are often explored as precursor molecules to produce new chemical entities/derivatives that are more effective and/or possess higher bioavailability [10,12]. Nonetheless, pure betulinic and oleanolic acids are difficult to obtain since they are structurally similar and occur simultaneously in different natural matrices [9]. As a result, their prices increase greatly with increasing purity.

Qualitative and quantitative analysis of TTAs rich-extracts has been performed by multiple methods such as thin-layer chromatography, capillary electrophoresis, gas chromatography, and supercritical fluid and liquid chromatography [13]. Among these, gas chromatography and high-performance liquid chromatography (HPLC) remain the most widely used techniques for TTAs analysis [4]. HPLC is frequently considered as it allows direct and simple analysis without derivatization steps. Moreover, it can be easily scaled-up for the preparative chromatographic separation/isolation of individual compounds with high throughput and purity [14], provided that the stationary phase, eluent and chromatographic conditions are properly selected and optimized. As a result of the lack of ultraviolet (UV) chromophores in TTAs structures, and consequent low UV absorbance, detection in HPLC analysis is often performed at wavelengths between *ca.* 200 and 210 nm to avoid interference between solutes and mobile phase, or by using different detection systems such as evaporative light scattering detection (ELSD) [15,16], mass spectrometry (MS) [17,18], and fluorescence detection (FLD) after precolumn derivatization with adequate labeling markers [19–22].

Regarding stationary phases for the separation of betulinic and oleanolic acids, octadecylsilyl bonded phases (ODS or C18) have undoubtedly received the most attention thus far with multiple C18 stationary phases with distinct endcapping treatments, pore sizes, surface area, and carbon loadings reported to conduct this separation, namely, Zorbax Eclipse Plus columns (150 x 3 – 4.6 mm, 1.8 – 3.5 µm) [17,18], polymeric Zorbax Eclipse PAH C18 columns (150 x 4.6 mm, 3.5 µm) [23,24], LiChrospher C18 columns (250 × 4.6 mm, 5 µm) [25,26], Hypersil BDS and ODS C18 columns (250 × 4.6 mm, 5 µm) [15,27], Symmetry C18 columns (250 × 4 mm, 5 µm) [28], Luna C18 columns (250 × 4.6 mm, 5 µm) [29], Spherisorb C18 columns (250 × 4.6 mm, 5 - 10 µm) [30], core-shell Kinetex C18 columns (250 × 4.6 mm, 5 µm) [31], Apollo C18 (250 × 4.6 mm, 5 µm) [30], Acquity UPLC HSS C18 columns [32,33], among others. Frequently, the separation conditions reported in the previous works did not ensure baseline separation (low selectivity and resolution) and/or relied heavily on acetonitrile based mobile phases modified

with water. This fact penalizes the preparative chromatographic process productivity taking into account the low solubilities of these triterpenic acids in acetonitrile and water [30,34].

Apart from C18 phases, porous Graphitic columns (PGCs) [35] revealed to be promising candidates for triterpenoids separation. For instance, Bérangère *et al*. [16] reported for the first time the use of PGCs for the separation of five triterpenic acids, including betulinic and oleanolic acids. A Hypercarb column (150 x 4.6 mm, 5 µm) with solvent mixtures of different compositions of acetonitrile/chloroform, acetonitrile/methylene chloride, acetonitrile/methyl tert-butyl ether, and methanol/methyl tert-butyl ether was tested and high selectivities were obtained. More recently, Rhourri-Frih *et al*. [36] and Grigoras *et al.* [37] performed the separation of multiple triterpenoids with Hypercarb columns: a column with 100 x 2.1 mm, (5 µm) with gradients of acetonitrile/isopropanol, and a column with 50 x 4.6 mm, (5 µm) with gradients of methanol/acetonitrile/isopropanol, respectively. In both works, clear baseline separation between betulinic and oleanolic acids was achieved. Despite their promising results, PGCs utilization may be limited from variability and general loss of retention over time [38], and because they are not so available in the market as C18 and other bonded phases are.

Mixed-mode or multimode chromatography is a chromatographic method in which at least two separation mechanisms contribute actively for solutes retention. It has become increasingly popular as an alternative or complementary tool due to its unique selectivity and retention of a variety of compounds [39,40]. Recently, Falev *et al*. [18] compared the performance of five distinct columns to conduct the separation of 10 pentacyclic triterpenoids: an Acclaim Mixed-Mode WAX-1 with embedded amide and terminal tertiary amino groups (150 x 2.1 mm, 3 µm), a Zorbax Eclipse Plus C18 and Zorbax Stable Bond Aq (150 x 3 mm, 3.5 µm), a Nucleodur PolarTec with embedded amide groups (150 x 2 mm, 1.8 µm), and a Nucleodur HILIC with a zwitterionic sulfobetaine stationary phase (150 x 3 mm, 3 µm). The best separation results were obtained with the Acclaim Mixed-Mode WAX-1 column and a mobile phase of

acetonitrile/water 85/15 (%, v/v) (33.3 mM aqueous formate buffer, pH 4). The remaining columns failed to provide baseline separation with the tested mobile phases.

Since their introduction in liquid chromatography [41–43], triacontylsilyl (C30) bonded phases have proved to be effective adsorbents in the analysis of plant extracts, food samples, biological tissues and synthetic mixtures of carotenoids and geometric isomers [44,45]. Moreover, they are known to provide higher sample loadings and more reproducible retention behavior than C18 phases when operated in highly aqueous solvent environments [44,46]. Recently, a comparison between multiple monomeric and polymeric C30 and C18 stationary phases was accomplished by Sander *et al*. [47] and better separations of carotenoid isomers were obtained with C30 columns than with C18 columns.

It is known that C30 stationary phases, particularly the Acclaim C30 ones, provide good selectivities for triterpenic acids fractionation [48], but for the specific betulinic and oleanolic acids separation very limited work is available related to mobile phase selection. Therefore, this work focused the isolation of these TTAs with the packing material of an Acclaim C30 column (250 × 4.6 mm, 5 μm). Methanol, water, acetonitrile, ethanol, isopropanol, ethyl acetate, acetone and mixtures thereof were isocratically tested to select the best mobile phase (in terms of compromise between selectivity, resolution and TTAs solubility) to be used in a preparative simulated moving bed (SMB) separation. The method of moments was adopted to quickly determine the isotherms, the axial dispersion coefficients, and the global linear driving force coefficients of each acid. Afterwards, these parameters were successfully validated modeling unary and binary breakthrough curves, and were used in a general optimization strategy based on design of experiments – response surface methodology (DoE-RSM) [49] to find the best SMB operating conditions for their isolation. Lastly, water was investigated as precipitation agent for the recovery of these TTAs from the raffinate and extract streams. With this purpose, the solubility of each acid was measured in methanol/acetonitrile 70/30, 50/50, and 30/70 (%, v/v) modified with increasing water contents up to 65 % (%, v/v).

2. Modeling

2.1. Single column and SMB modeling and optimization

The modeling of breakthrough curves (single column) and simulated moving bed (SMB) unit was performed using the chromatographic model considering axial dispersion plug flow pattern ($D_{\mathrm{ax,ij}}$), and internal and external mass transfer resistances lumped into a global linear driving force coefficient ($K_{\mathrm{LDF,ij}}$) given by Ruthven [50]:

$$\frac{\partial C_{\mathrm{ij}}}{\partial t} = D_{\mathrm{ax,ij}}\frac{\partial^2 C_{\mathrm{ij}}}{\partial z^2} - v_{\mathrm{j}}\frac{\partial C_{\mathrm{ij}}}{\partial z} - \frac{1-\varepsilon_{\mathrm{b}}}{\varepsilon_{\mathrm{b}}}K_{\mathrm{LDF,ij}}(q_{\mathrm{ij}}^{*} - q_{\mathrm{ij}}) \quad (1)$$

$$\frac{\partial q_{\mathrm{ij}}}{\partial t} = K_{\mathrm{LDF,ij}}(q_{\mathrm{ij}}^{*} - q_{\mathrm{ij}}) \quad (2)$$

where t and z are the time and spatial coordinates, C_{ij} is the concentration of species i in the liquid bulk of column j, q_{ij} is the average concentration of species i in the adsorbent of column j , v_{j} is the interstitial fluid velocity in column j, and ε_{b} is the bed porosity. A linear isotherm was assumed to describe the equilibrium between the solid (q_{ij}^{*}) and liquid (C_{ij}) phases:

$$q_{\mathrm{ij}}^{*} = H_{\mathrm{i}}C_{\mathrm{ij}} \quad (3)$$

where H_{i} is the distribution coefficient of species i. Equations (1) and (2) were subjected to proper initial and Dankwerts boundary conditions. More details regarding the SMB modeling may be found elsewhere [49,51]. The SMB optimization was performed following the design of experiments and response surface methodology (DoE-RSM) approach reported by Aniceto *et al*. [49]. In summary, a grid of 13 simulation points in the plane $m_{\mathrm{II}} \times m_{\mathrm{III}}$ (SMB dimensionless flow rates; the factors of DoE-RSM) was defined and the responses – the extract and raffinate purities (PuX, and PuR, respectively) and SMB productivity ($Prod$) – were used to define the multi-objective optimization: minimum purity of 99 % in raffinate and extract while maximizing productivity. Quadratic models were selected for PuX and PuR, and a linear model was the default for $Prod$. The dimensionless flow rates m_{I} and m_{IV} were fixed with a safety margin from

the point of minimum solvent consumption given by the Triangle Theory [52]. For a binary mixture, purity (PuX and PuR) is defined for both streams according to the desired product in each outlet:

$$PuX\ (\%) = 100\frac{C_{\mathrm{A}}^{\mathrm{X}}}{C_{\mathrm{A}}^{\mathrm{X}} + C_{\mathrm{B}}^{\mathrm{X}}}\ ;\ PuR(\%) = 100\frac{C_{\mathrm{B}}^{\mathrm{R}}}{C_{\mathrm{A}}^{\mathrm{R}} + C_{\mathrm{B}}^{\mathrm{R}}} \tag{4}$$

where A is the most retained component, B is the less retained component, and superscripts X and R denote extract and raffinate, respectively. Productivity ($Prod$) is defined as the amount of feed mixture processed per unit volume of stationary phase and per unit time:

$$Prod\ (\mathrm{kg}/(\mathrm{m}^3_{\mathrm{adsorbent}}\ \mathrm{day})) = \frac{Q_{\mathrm{F}}\left(C_{\mathrm{A}}^{\mathrm{F}} + C_{\mathrm{B}}^{\mathrm{F}}\right)}{V_{\mathrm{T}}} \tag{5}$$

where superscript F denotes feed stream, Q is the volumetric feed flow rate, and V_{T} is the total volume of stationary phase in all SMB columns. Solvent consumption (SC) is also provided as an additional performance indicator (but not used in the multi-objective optimization), and is given by:

$$SC(\mathrm{m}^3/\mathrm{kg}) = \frac{Q_{\mathrm{E}} + Q_{\mathrm{F}}}{Q_{\mathrm{F}}(C_{\mathrm{A}}^{\mathrm{F}} + C_{\mathrm{B}}^{\mathrm{F}})} \tag{6}$$

where subscript E denotes eluent.

2.2. Moment analysis

The moment analysis is one of the simplest strategies to determine equilibrium and kinetic model parameters, since it requires only a series of impulse experiments to be performed at different flow rates [14,53,54], thus reducing chemicals consumption and workload. The equations for the first ($\mu_{1,\mathrm{i}}$) and second ($\mu_{2,\mathrm{i}}$) moments for a given species i are given by equations (7) and (8), respectively [55]:

$$\mu_{1,\mathrm{i}} = t_{\mathrm{r,i}} = \frac{L}{v}\left(1 + \frac{1-\varepsilon_{\mathrm{b}}}{\varepsilon_{\mathrm{b}}}H_{\mathrm{i}}\right) \tag{7}$$

$$\mu_{2,\mathrm{i}} = \frac{2L}{v}\left[\frac{D_{\mathrm{ax,i}}}{v^2}\left[1 + \frac{1-\varepsilon_\mathrm{b}}{\varepsilon_\mathrm{b}}H_\mathrm{i}\right]^2 + \left(\frac{1-\varepsilon_\mathrm{b}}{\varepsilon_\mathrm{b}}\right)\frac{H_\mathrm{i}}{K_{\mathrm{LDF,i}}}\right] \tag{8}$$

where $t_{\mathrm{r,i}}$ is the mean residence time of species i, and L is the column length. The axial dispersion coefficient may be estimated by [56]:

$$D_{\mathrm{ax,i}} = 0.73D_{\mathrm{m,i}} + 0.5d_\mathrm{p}v \tag{9}$$

where $D_{\mathrm{m,i}}$ and d_p are the molecular diffusion and particle diameter, respectively. The expression for the height equivalent to a theoretical plate ($HETP_\mathrm{i}$) may be determined as function of the first and second moments and is given by equation (10) [55]:

$$HETP_\mathrm{i} = \frac{L}{N_\mathrm{i}} = \frac{\mu_2}{\mu_1^2}L = \frac{2D_{\mathrm{ax,i}}}{v} + 2v\left(\frac{\varepsilon}{1-\varepsilon}\right)\frac{1}{H_\mathrm{i}K_{\mathrm{LDF,i}}}\left(1 + \frac{\varepsilon}{(1-\varepsilon)\mathrm{H_i}}\right)^{-2} \tag{10}$$

where $N_\mathrm{i} = 5.545\left(t_{\mathrm{r,i}}/w_{0.5\mathrm{He,i}}\right)^2$ is the number of theoretical plates of the column, and $w_{0.5\mathrm{He,i}}$ the peak width at half height.

In this work, the equilibrium and transport parameters were determined as follows: (i) the first moment (equation (7)) was used to adjust the distribution coefficient (H_i); and (ii) equation (10) was fitted to the experimental $HETP_\mathrm{i}$ curve to obtain the axial dispersion ($D_{\mathrm{ax,i}}$) and global linear driving force ($K_{\mathrm{LDF,i}}$) coefficients. All fittings were performed using the Nelder-Mead simplex method and the least squares objective function. The average absolute relative deviation ($AARD, \%$) was always calculated in order to access the goodness of the fittings and quality of the predictions; for a generic function y it is given by:

$$AARD\ (\%) = \frac{100}{NDP}\sum_{i=1}^{NDP}\left|\frac{y^{\mathrm{calc}} - y^{\mathrm{exp}}}{y^{\mathrm{exp}}}\right|_\mathrm{i} \tag{11}$$

where superscripts calc and exp denote calculated and experimental values, and NDP is the number of data points. The chromatographic model (equations (1) and (2)) was numerically solved in Matlab using the method of lines through the *pdepe* function.

3. Experimental section

3.1. Reagents and materials

HPLC grade methanol and isopropanol were purchased from Sigma-Aldrich; acetonitrile, ethanol, and water were purchased from Carlo Erba Reagents; and ethyl acetate and acetone were purchased from VWR. Betulinic acid (purity ≥ 98 %) and oleanolic acid (purity ≥ 98 %) were purchased from AK Scientific. All solvents and solutes were used as purchased without further purification. An Acclaim C30 column (250 × 4.6 mm, $d_{\mathrm{p}} = 5$ μm, pore size: 200 Å, surface area: 200 m^2/g, carbon load: 13 %, monomeric bonded phase) was purchased from Thermo Fisher Scientific, Inc.

3.2. High pressure liquid chromatography (HPLC) setups

Chromatographic experiments were performed in three different equipments: (i) a Gilson HPLC system equipped with a 305 isocratic controller pump, a 306 gradient pump, a 805 manometric module, a 811C dynamic mixer, and a 118 UV/Vis detector; (ii) a Gilson HPLC system equipped with a 131 refractive index detector and a 307 isocratic pump; and (iii) a Thermo Scientific™ Dionex™ UltiMate™ 3000 UHPLC system equipped with a Dionex™ UltiMate™ 3000 pump, a Dionex™ UltiMate™ 3000 column compartment and a Dionex™ UltiMate™ 3000 diode array detector. The Gilson Unipoint Software version 5.11 (Gilson, Inc., Middleton, WI, USA) was used to record automatically all the chromatographic runs performed in the Gilson systems, and the Thermo Scientific™ Dionex™ Chromeleon™ 7 software was used for the chromatographic runs in the UltiMate 3000 UHPLC equipment.

3.3. Mobile phase selection

Impulse experiments were conducted to select a suitable mobile phase to perform the chromatographic separation of betulinic and oleanolic acids. Small injections of 20 µL of feed solutions consisting of binary mixtures of betulinic and oleanolic acids were performed at room temperature (23 °C) on the Gilson HPLC systems at a flow rate of 0.40 mL/min. When the mobile phase consisted exclusively of methanol, water, acetonitrile, or any other mixture consisting solely of these solvents, the HPLC system equipped with the UV/Vis detector was used at 210 nm and the concentrations of betulinic and oleanolic acids in the feed mixture were 0.0980 and 0.102 mg/mL, respectively. When mobile phase contained ethanol, isopropanol, ethyl acetate, acetone, or any mixture containing at least one of these solvents, the HPLC system equipped with the refractive index detector was adopted, and the concentrations of betulinic and oleanolic acids in the feed mixture were in the range of 0.245 – 0.515 mg/mL and 0.250 – 0.550 mg/mL, respectively. The solvent used in the reference cell of the refractive index detector was always the mobile phase being investigated in a given experiment.

When testing a different mobile phase, the injection of betulinic and oleanolic acids standards was always performed to identify the corresponding peaks in their binary mixtures.

3.4. Moment analysis experiments

For the determination of the first moments and $HETP$ curves of betulinic and oleanolic acids, a series of impulse experiments (20 µL injections) of each acid at room temperature (23 °C) were performed in the Thermo Scientific™ Dionex™ UltiMate 3000 UHPLC with an Acclaim C30 column. Injections were performed at different flow rates ranging from 0.20 mL/min (the minimum recommended by the equipment manufacturer) up to 1.00 mL/min with a mobile phase of methanol/acetonitrile 50/50 (%, v/v). Injected concentrations of betulinic and oleanolic

acids were, respectively, 0.152 and 0.169 mg/mL. UV detection was set at 210 nm and for each flow rate at least duplicate injections were performed for each acid.

3.5. Unary and binary breakthrough adsorption experiments

Unary and binary breakthrough curves were measured in a custom laboratorial installation as follows: after equilibrating the column (Acclaim C30 (250 x 4.6mm, 5 µm)) with the mobile phase (methanol/acetonitrile 50/50 (%, v/v)), a feed solution of known concentration was continuously introduced into the column (step signal) until equilibrium (adsorption stage). After that, the desorption stage was initiated by switching the feed pump for the mobile phase pump (both Knauer Azura® P 4.1S pumps). Samples were collected periodically throughout the adsorption and desorption stages and were later analyzed by HPLC to determine the full breakthrough curves. Unary breakthroughs were determined with a feed concentration in the range of 0.1991 – 1.991 mg/mL for betulinic acid and in the range of 0.1989 – 1.989 mg/mL for oleanolic acid. One binary breakthrough curve with a feed concentration of 0.661 and 0.835 mg/mL for betulinic and oleanolic acids, respectively, was also determined. The cumulative volume of tubing and fittings of the system (*i.e.,* extra column volume) was found to be 0.381 mL. All curves were determined at a flow rate of 1.00 mL/min and at room temperature (23 °C).

3.6 Solubility measurements

The solubility measurements of betulinic and oleanolic acids in distinct solvents were carried out following the classical saturation shake-flask method [57]. The solvents were methanol/acetonitrile 70/30, 50/50 and 30/70 (%, v/v) mixtures, and each one was modified adding water from 0 up to 65 % (v/v). An excess of each TTA was placed in a glass capped vial containing ca. 20 mL of the methanol/acetonitrile/water mixture in order to obtain a saturated solution. The mixture was allowed to equilibrate for at least 72 hours at constant temperature (23 °C), after which the supernatant solution was filtered using a 0.45 µm cellulose membrane

and analyzed by HPLC to determine the TTA concentration. Several measurements were carried out during 3 days to confirm that the system was under equilibrium.

4. Results and discussion

4.1. Selection of mobile phase

The ability of the packing material of the Acclaim C30 column (250 × 4.6 mm, 5 µm) to separate betulinic and oleanolic acids was carefully assessed by testing different eluents as described in section 3.3 (methanol, water, acetonitrile, ethanol, isopropanol, ethyl acetate, acetone and mixtures thereof). The obtained selectivity and resolution values for all mobile phases (identified from A to O) are listed in Table 1 and the respective chromatograms are shown in Figure 1. In all cases betulinic acid was firstly eluted followed by oleanolic acid.

Increasing the size of the alcohol aliphatic chain – from methanol to ethanol and isopropanol (chromatograms A, I and M, respectively) – the separation of betulinic and oleanolic acids suffered a severe selectivity decrease, occurring co-elution of both acids for ethanol and isopropanol ($S_{\mathrm{OA,BA}} = 1.00$). Notwithstanding this TTAs co-elution, some adsorption takes place because their retention times were higher than the space time (7.26 min). Modifying the methanol with water as well as with acetonitrile, the selectivity and resolution increased by increasing the amount of modifier, reaching a selectivity ($S_{\mathrm{OA,BA}}$) value of 1.24 and a resolution ($R_{\mathrm{OA,BA}}$) of 3.70 for methanol/acetonitrile 30/70 (%, v/v) (chromatogram G). Noteworthy is also the higher sensitivity of the separation to small increments of water than acetonitrile, since retention times of betulinic and oleanolic acids more than doubled after 10 % (v/v) water addition in comparison with pure methanol. A mixture of methanol/acetone 50/50 (%, v/v) (chromatogram H) was also tested in this work and a value of $S_{\mathrm{OA,BA}} = 1.20$ was obtained due to lower retention times in comparison with, for example, pure methanol. Nonetheless, the chromatographic peaks were severely overlapped.

The modification of ethanol and isopropanol with acetonitrile resulted equally in the improvement of TTAs isolation, particularly for ethanol for which $S_{\mathrm{OA,BA}} = 1.17$ for ethanol/acetonitrile 50/50 (%, v/v) (chromatogram L). Lastly, pure ethyl acetate (chromatogram O) was used without success as both TTAs co-eluted together. Overall, better separations of betulinic and oleanolic acids were achieved with binary mixtures of methanol and acetonitrile (higher selectivities and resolutions).

Table 1 – Impulse experiments for the selection of a mobile phase for the separation of betulinic (BA) and oleanolic (OA) acids. Column: Acclaim C30 (250 × 4.6 mm, 5 µm), flow rate of 0.40 mL/min and room temperature (23 °C).

Mobile Phase (%, v/v)		Selectivity ($S_{\mathrm{OA,BA}}$) [(a)]	Resolution ($R_{\mathrm{OA,BA}}$) [(b)]
UV-vis detection			
A	Methanol	1.16	1.85
B	Methanol/Water (95/5)	1.18	2.41
C	Methanol/Water (90/10)	1.20	2.62
D	Methanol/Acetonitrile (85/15)	1.19	2.36
E	Methanol/Acetonitrile (70/30)	1.22	2.94
F	Methanol/Acetonitrile (50/50)	1.23	3.35
G	Methanol/Acetonitrile (30/70)	1.24	3.70
Refractive index detection			
H	Methanol/Acetone (50/50)	1.20	[(c)]
I	Ethanol	1.00	0.00
J	Ethanol/Water (90/10)	1.15	[(c)]
K	Ethanol/Acetonitrile (85/15)	1.15	[(c)]
L	Ethanol/Acetonitrile (50/50)	1.17	1.55
M	Isopropanol	1.00	0.00
N	Isopropanol/Acetonitrile (50/50)	1.08	0.98
O	Ethyl Acetate [(d)]	1.00	0.00

[(a)] $S_{\mathrm{i,j}} = k'_{\mathrm{i}}/k'_{\mathrm{j}}$ where k'_{i} is the retention factor of i given by $k'_{\mathrm{i}} = {(t_{r,\mathrm{i}} - t_0)}/{t_0}$ with t_0 being the column hold-up time (7.26 min at 0.40 mL/min).

[(b)] $R_{\mathrm{i,j}} = 1.18(t_{\mathrm{r,i}} - t_{\mathrm{r,j}})/(w_{0.5\mathrm{He,i}} + w_{0.5\mathrm{He,j}})$

[(c)] Not possible to be determined due to extensive peak overlap.

[(d)] Flow rate of 0.30 mL/min.

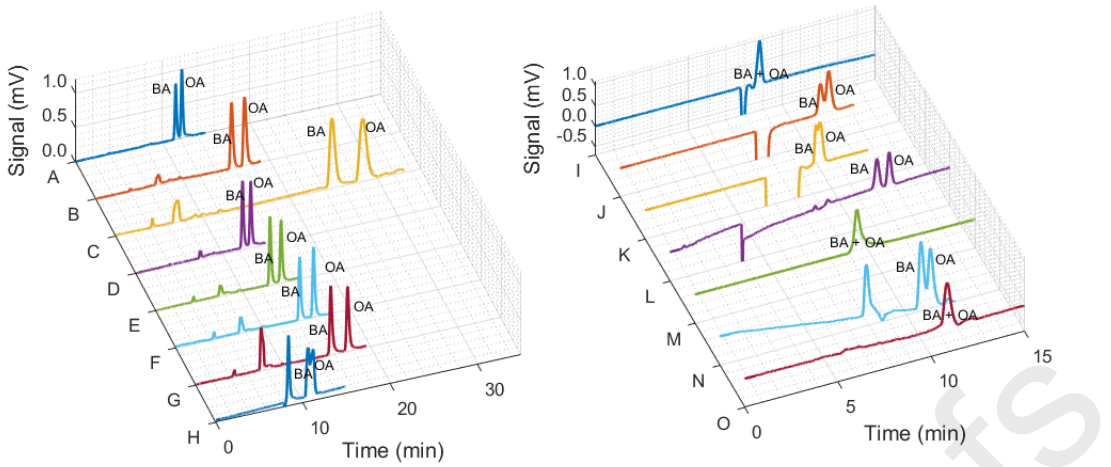

Figure 1 – Normalized chromatograms of the separation of betulinic (BA) and oleanolic (OA) acids. Column: Acclaim C30 (250 × 4.6 mm, 5 µm), flow rate of 0.40 mL/min, room temperature (23 °C) and UV detection of 210 nm. The mobile phase labels (A-O) correspond to those provided in Table 1.

The separation performance, in terms of selectivity, of the Acclaim C30 column studied in this work was compared with two C18 columns [17,30,58]. In these previous works, an Apollo C18 (250 x 4.6 mm, 5 µm) [30,58] column and a Zorbax Eclipse Plus C18 column (150 x 4.6, 1.8 µm) [17] were used for the separation of betulinic and oleanolic acids using binary solvent mixtures containing methanol/acetonitrile in different volumetric ratios. The retention factors for both acids and selectivities as function of acetonitrile content are represented in Figure 2a and Figure 2b, respectively. To calculate the selectivities from the data provided in the work of Olmo-García *et al.* [17], the column dead volume was determined from the elution time of thiourea (a common tracer used to determine column total porosity) which was obtained from reference [59] and found to be 1.08 mL. In this way, it was assumed that the packing features were identical in all Zorbax columns. Due to the various flow rates used with the different columns, the peak efficiencies (*i.e.*, height equivalent to a theoretical plate, $HETP$) were not considered for direct comparison. From Figure 2a it is possible to see that, for all columns, the retention factors (k') of betulinic and oleanolic acids increase with increasing acetonitrile content, being this effect more pronounced for the C18 columns which present higher slopes. The selectivities, for instance, growth at a decreasing rate for all columns with a transition zone around 50 %

(v/v) of acetonitrile, above which the selectivity increment is reduced. For small volumetric fractions of acetonitrile, a small variation in the mobile phase composition has a higher impact on selectivity than for higher acetonitrile contents. The packing of the Acclaim C30 column provided the highest separation selectivities when compared with both C18 columns, and the ratio of selectivities between C30 and C18 columns remained approximately constant and equal to 1.08 throughout the whole acetonitrile range. Regarding the Apollo and Zorbax Eclipse C18 columns, it is interesting to note how the selectivities seem to coincide. In fact, the Apollo C18 having 15 % of carbon distributed over an area of 340 m^2/g and an average pore diameter of 100 Å [60], and the Zorbax Eclipse Plus C18 column with a carbon load of 9 % distributed in *ca.* half the surface area (160 m^2/g) and average pore size of 95 Å [61] result approximately in the same density of octadecyl bonded chains. Regarding the packing material of the Acclaim C30 column, a carbon load of 13 % over a surface area of 200 m^2/g and average pore size of 200 Å (twice as large as the Apollo C18) are reported [62]. Considering all these factors, methanol/acetonitrile 50/50 (%, v/v) was selected as the best mobile phase candidate for the preparative separation of betulinic and oleanolic acids. Thus, in the next sections all data are reported for the Acclaim C30 column using methanol/acetonitrile 50/50 (%, v/v) as mobile phase at 23 °C.

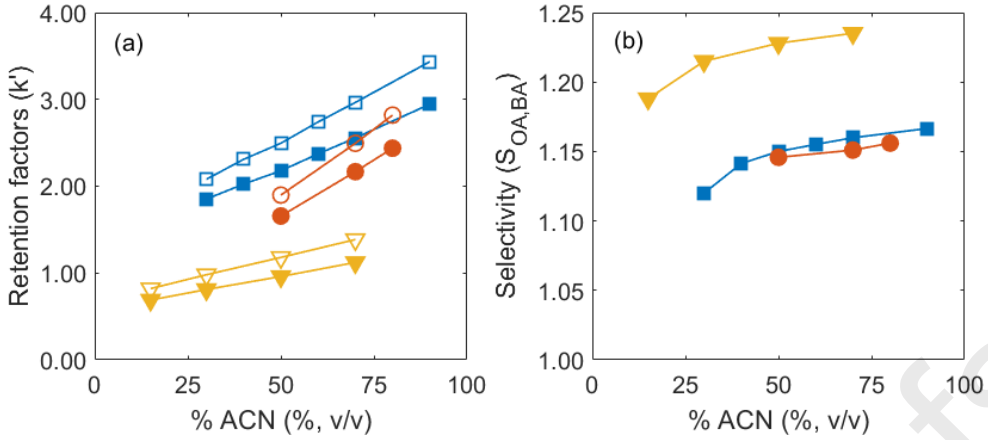

Figure 2 – (a) Retention factors (k') for betulinic (filled symbols) and oleanolic (open symbols) acids and (b) selectivities ($S_{\mathrm{OA,BA}}$) as function of acetonitrile content (%, v/v) in mobile phases consisting of binary mixtures of methanol/acetonitrile. Triangle symbols are the results from this work with the Acclaim C30 column; square symbols are results from the work of Olmo-García *et al*. [17] with a Zorbax Eclipse Plus C18 column (150 x 4.6 mm, 1.8 µm); and circles are the results from previous works [30,58] with an Apollo C18 column (250 x 4.6 mm, 5 µm).

4.2. Determination of equilibrium constants

The equilibrium constants of betulinic and oleanolic acids (for the Acclaim C30 column and methanol/acetonitrile 50/50 (%, v/v) at 23 °C) were determined experimentally using the first moment of the chromatographic model. According to equation (7), a series of impulse experiments were performed in the range of 0.20 and 1.00 mL/min and the retention times of each acid were recorded. The first moments for the two acids are plotted in Figure 3 and both linear fittings represent accurately the experimental points. The obtained equilibrium constants (H_{i}) for betulinic and oleanolic acids were 1.46 and 1.70 with $AARDs$ of 0.44 % and 0.45 %, respectively, and these values are compiled in Table 2.

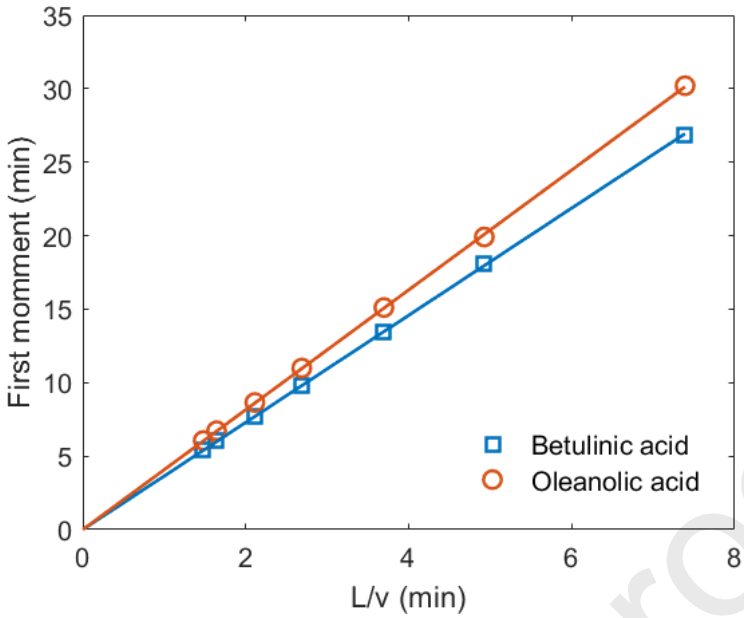

Figure 3 – First moment of betulinic (squares) and oleanolic (circle) acids *versus* the ratio of length to interstitial velocity of mobile phase. Column: Acclaim C30 (250 × 4.6 mm, 5 µm); mobile phase: methanol/acetonitrile 50/50 (%, v/v); temperature: 23 °C; UV detection: 210 nm. Symbols – experimental points; lines – first moment equation.

Table 2 – Equilibrium constants, molecular diffusivities, and global linear driving force coefficients of betulinic and oleanolic acids determined by the method of moments. Column: Acclaim C30 (250 × 4.6 mm, 5 µm); mobile phase: methanol/acetonitrile 50/50 (%, v/v); temperature: 23 °C; UV detection: 210 nm.

	Betulinic acid	Oleanolic acid
First moment		
H	1.46	1.70
$AARD$ (%)	0.436	0.450
HETP curves		
D_{m} (cm^2/min)	1.49×10^{-3}	1.01×10^{-3}
K_{LDF} (min^{-1})	9665	9179
$AARD$ (%)	1.68	1.17

4.3. Determination of axial dispersion and mass transfer coefficients

The combined effect of axial dispersion and internal/external mass transfer limitations is responsible for peak broadening and consequent reduction of column efficiency. The representation of HETP *versus* interstitial velocity of mobile phase is shown in Figure 4. The fittings (equation (10)) are in good agreement with the experimental points with $AARDs$ of 1.68 % and 1.17 % for betulinic and oleanolic acids, respectively, with the model slightly underestimating data near the minimum $HETP$, where column efficiency is maximum (flow rate of *ca.* 0.4 mL/min). Higher D_{m} and K_{LDF} coefficients were determined for betulinic acid, highlighting its smaller mass transfer limitations but higher axial dispersion in the range of studied experimental conditions. Overall, despite the smaller K_{LDF}, the number of theoretical plates associated to oleanolic acid chromatographic peaks is higher than betulinic acid due the combined effect of higher retention time and lower axial dispersion. The obtained D_{m} and K_{LDF} coefficients for betulinic and oleanolic acids are compiled in Table 2 with the respective $AARDs$.

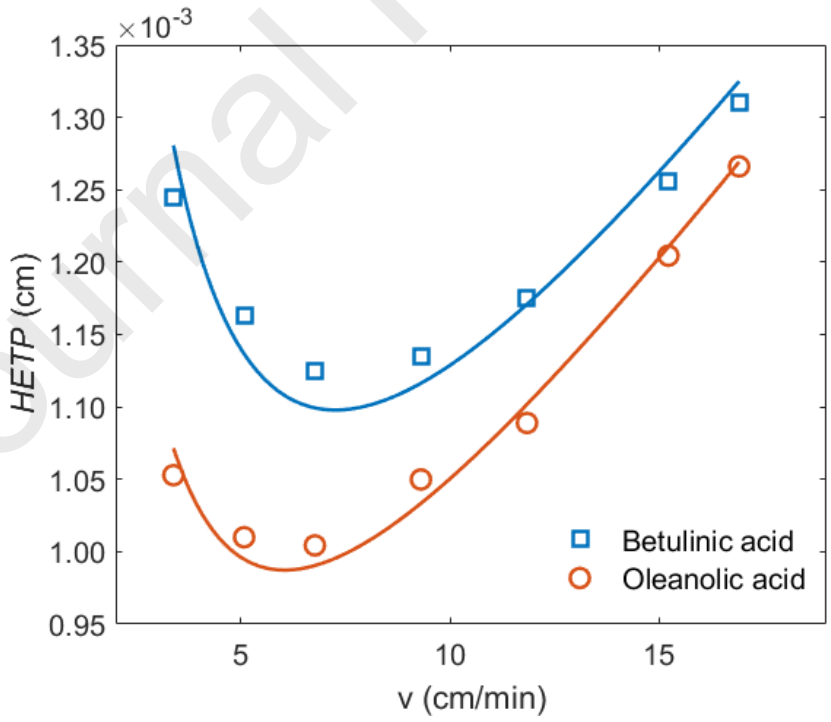

Figure 4 – HETP of betulinic (squares) and oleanolic (circle) acids as function of interstitial velocity of mobile phase. Column: Acclaim C30 (250 × 4.6 mm, 5 μm); mobile phase:

methanol/acetonitrile 50/50 (%, v/v); temperature: 23 °C; UV detection: 210 nm. Symbols – experimental points; lines – HETP model (equation (10)).

4.4. Modeling of unary and binary breakthrough curves

The parameters previously determined by the method of moments were validated modeling independent breakthrough curves of pure betulinic and pure oleanolic acids, and one breakthrough curve of a binary mixture of both acids with the chromatographic model.

The unary breakthroughs were determined up to close the limit of solubility of each acid [30], in the range of 0.1991 – 1.991 mg/mL for betulinic acid and 0.1989 – 1.989 mg/mL for oleanolic acid, at 23 °C and flow rate of 1.00 mL/min. The experimental and modeling results of the adsorption and desorption stages for betulinic and oleanolic acids are plotted in Figure 5 and Figure 6, respectively. Overall, good agreement between data and model was obtained, with $AARDs$ of 10.7 % and 9.61 % for betulinic and oleanolic acids, respectively. The results also confirmed that the assumption of linear isotherms in the analysis of the first moments was correct. Moreover, the extrapolation of the linear isotherms up to close the solubility of each acid to describe the dynamic adsorption behavior in single column was also accurate. Regarding axial dispersion and mass transfer coefficients, the relatively low dispersion (5.32×10^{-3} and 4.97×10^{-3} cm^2/min for betulinic and oleanolic acids, respectively, at 1.00 mL/min) and high mass transfer coefficients were able to describe accurately the sharp front and rear sides of all breakthroughs, evidencing small deviations to the ideal adsorption behavior (i.e., negligible axial mixing effects and mass transfer resistances). This emphasizes the high efficiency of the Acclaim C30 packing material and places it in stark contrast with the packing material of the Apollo C18 column (250 × 4.6 mm, 5 μm), for which the mass transfer coefficients obtained for methanol/acetonitrile 50/50 (%, v/v) were 28.8 and 11.7 min^{-1} for betulinic and oleanolic acids, respectively [30].

To further evaluate possible competitive effects and to validate the extension of the determined parameters to SMB operation, a breakthrough curve of a binary mixture of betulinic (0.661 mg/mL) and oleanolic (0.835 mg/mL) acids was measured in the same way as those carried out for pure acids. Nonetheless, lower individual concentrations of each acid were employed in order to avoid possible precipitation issues in real SMB operation, maintaining the total concentration (1.496 mg/mL = 0.661 + 0.835 mg/mL) below the saturation of each individual compound (taking into account they are isomers). The experimental and modeling results are plotted in Figure 7. Once again, good agreement between the experimental and calculated results is observed with $AARDs$ of 8.37 % and 11.9 % for betulinic and oleanolic acids, respectively. The results demonstrated the absence of competitive effects and thus validated the application of the previously obtained parameters (from the method of moments applied to the pure solutes) to the modeling of the separation of betulinic and oleanolic acids mixtures by SMB.

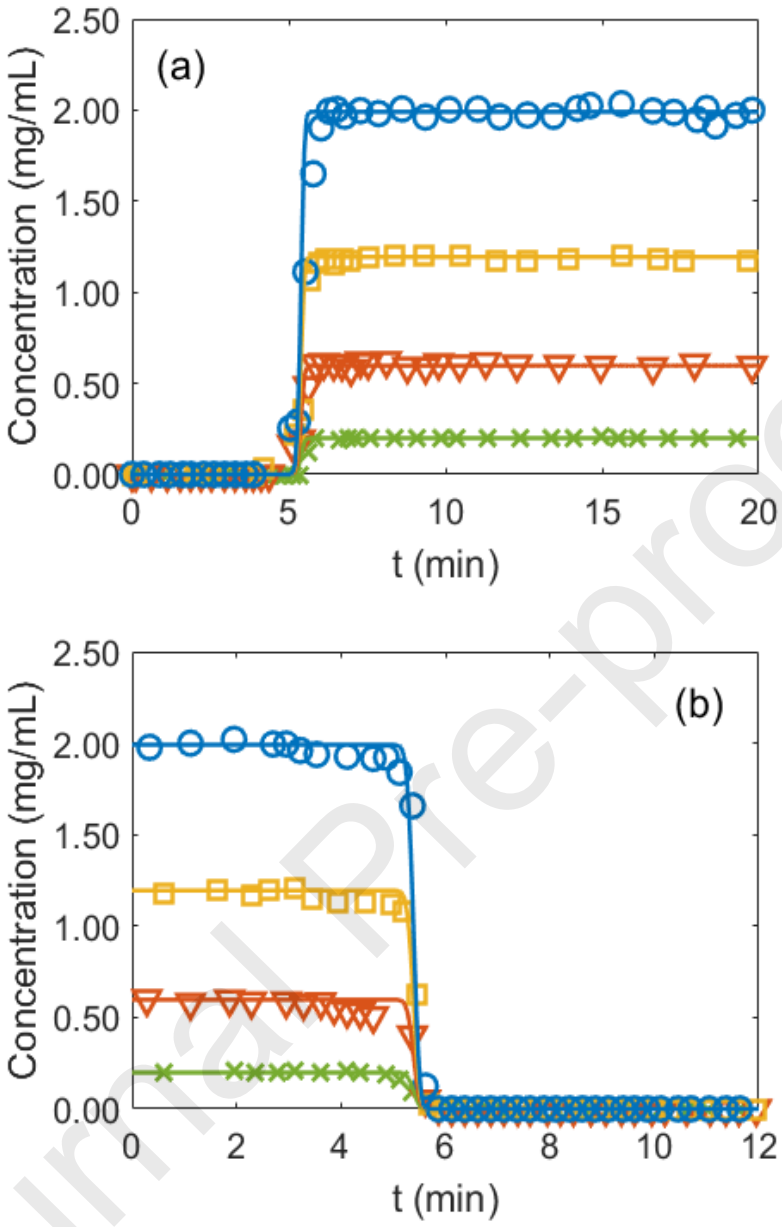

Figure 5 – Breakthrough curves of pure betulinic acid at different feed concentrations with the packing material of the Acclaim C30 column and methanol/acetonitrile 50/50 (%, v/v) as mobile phase. (a) – adsorption stage; (b) – desorption stage. Flow rate of 1.00 mL/min and temperature of 23 °C. Symbols – experimental points; lines – chromatographic model.

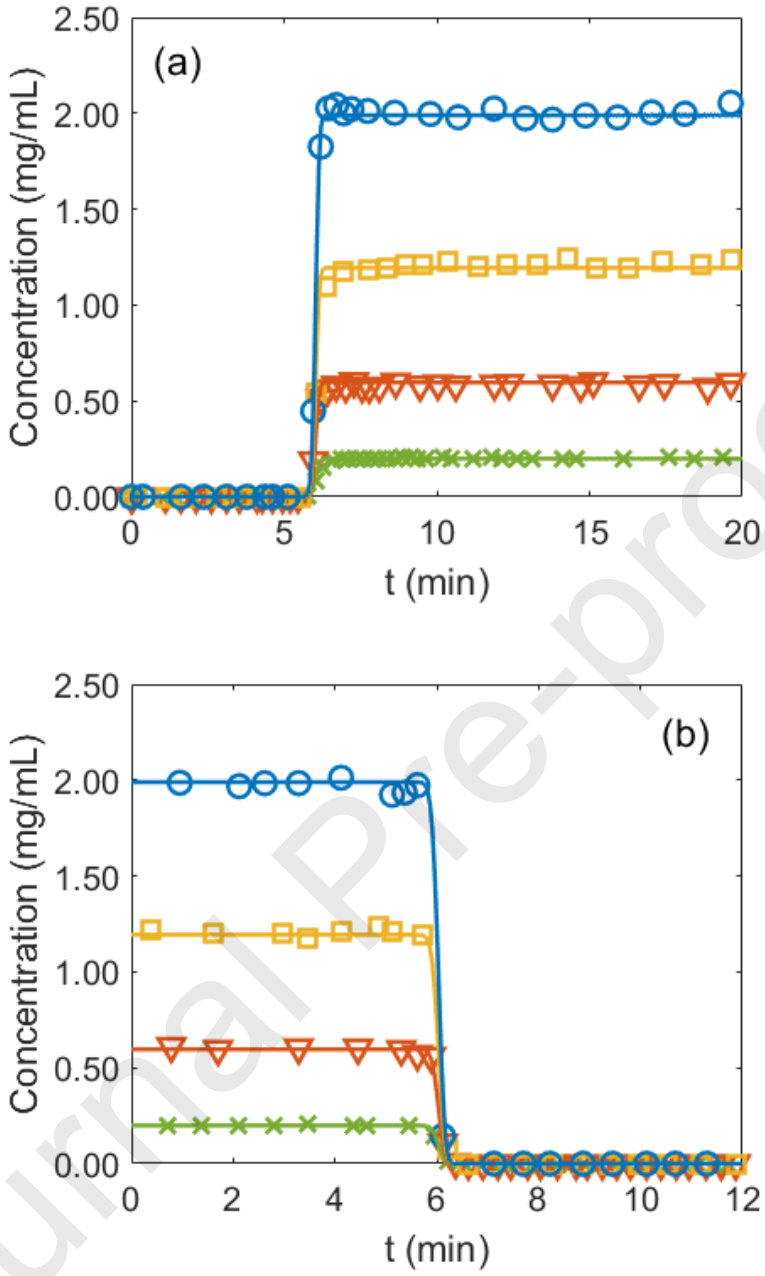

Figure 6 – Breakthrough curves of pure oleanolic acid at different feed concentrations with the packing material of the Acclaim C30 column and methanol/acetonitrile 50/50 (%, v/v) as mobile phase. (a) – adsorption stage; (b) – desorption stage. Flow rate of 1.00 mL/min and temperature of 23 °C. Symbols – experimental points; lines – chromatographic model.

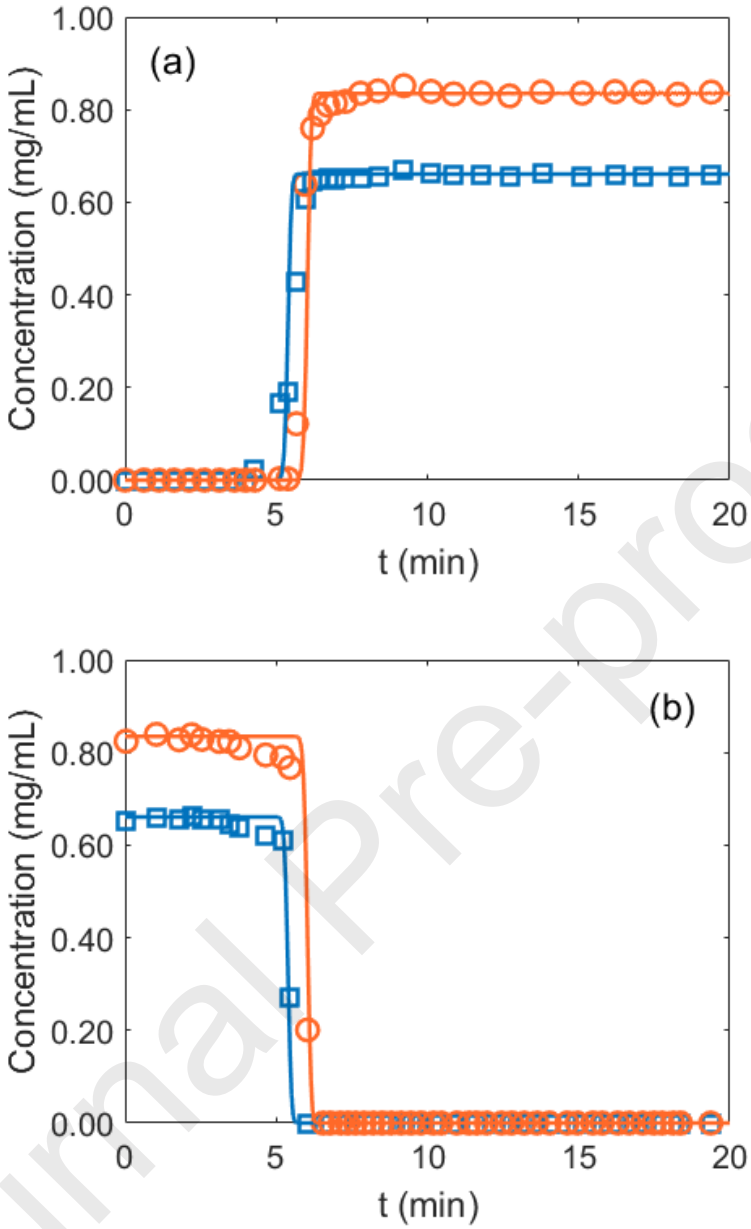

Figure 7 – Binary breakthrough curves of betulinic (squares, feed concentration = 0.661 mg/mL) and oleanolic (circles, feed concentration = 0.835 mg/mL) acids with the packing material of the Acclaim C30 column and methanol/acetonitrile 50/50 (%, v/v) as mobile phase. (a) – adsorption stage; (b) – desorption stage. Flow rate of 1.00 mL/min and temperature of 23 °C. Symbols – experimental points; lines – chromatographic model.

4.5. SMB simulations

With the equilibrium and kinetic parameters previously determined and thoroughly validated, simulated moving bed (SMB) simulations were carried out to assess the performance of a classical SMB with four sections and one column per section configuration (1-1-1-1) for the separation of betulinic and oleanolic acids. The packing material of the Acclaim C30 column was considered and the dimensions of the four columns used in the simulations were 75 x 22 mm (L x ID), 5 µm. It was assumed that all packing features (*e.g.*, porosities) and equilibrium and global linear mass transfer coefficients were the same for all columns. Since the film resistance to mass transfer was negligible, both $K_{\mathrm{LDF,BA}}$ and $K_{\mathrm{LDF,OA}}$ were always independent of flow rate. Moreover, extra column volumes were not considered for simplicity. The composition of the SMB feed mixture was defined considering: (i) The mass fractions of betulinic ($w_{\mathrm{BA}} = 0.20$) and oleanolic ($w_{\mathrm{OA}} = 0.25$) acids in extracts of triterpenic acids from *Eucalyptus globulus* bark obtained by solid-liquid and supercritical fluid extraction processes [63,64]; *E. globulus* bark is the most abundant biomass residue in Portugal pulp and paper industries. (ii) The solubility of betulinic and oleanolic acids in the mobile phase selected, methanol/acetonitrile 50/50 (%, v/v) [30]. Taking into account both sources of data, a total TTAs concentration of 2 mg/mL, resulting in 0.889 and 1.11 mg/mL of betulinic and oleanolic acids, respectively, was considered the feed mixture to the SMB.

The flow rate in section I (Q_{I}) is the highest in the SMB and was established according to the maximum superficial velocity recommended by Thermo Fisher Scientific Inc. for the Acclaim C30 columns [65]. Hence, for the maximum recommended superficial velocity of 9.03 cm/min and the aforementioned semi-preparative column dimensions, the flow rate $Q_{\mathrm{I}} =$ 34.3 mL/min was obtained, resulting in a pressure drop of 27.1 bar. This, for instance, is in contrast with previous works [30] for which the multi-position valve system was considered the limiting factor of the system, imposing a maximum pressure drop of 34 bar. All data necessary to conduct simulations are provided in Table 3.

Table 3 - Simulation parameters for the separation of betulinic (BA) and oleanolic (OA) acids by SMB. Adsorbent: packing of Acclaim C30 column; mobile phase: methanol/acetonitrile 50/50 (%, v/v); temperature of 23 °C.

System parameter	Value
Column configuration	1-1-1-1
L (cm)	7.5
ID (cm)	2.2
d_p (μm)	5
ε_b [(a)]	0.356
C_{BA}^F(mg/mL)	0.889
C_{OA}^F(mg/mL)	1.11
H_{BA}	1.46
H_{OA}	1.70
$D_{ax,BA,j}$ (cm²/min)	$1.09 \times 10^{-3} + 2.5 \times 10^{-4} v_j$
$D_{ax,OA,j}$ (cm²/min)	$7.40 \times 10^{-4} + 2.5 \times 10^{-4} v_j$
$K_{LDF,BA}$ (min^{-1}) [(b)]	9665
$K_{LDF,OA}$ (min^{-1}) [(b)]	9179
Q_I (mL/min)	34.3

(a) Taken from reference [66].

(b) The K_{LDF} values are equal for all SMB sections since the external mass transfer limitations are negligible.

The optimization of the betulinic and oleanolic acids separation was conducted employing a DoE-RSM approach previously reported by the authors [49]. An optimization grid with thirteen points encompassing the separation region provided by the Triangle Theory was created considering two factors, namely, the dimensionless flow rates in section II (m_{II}) and section III (m_{III}). Regarding the dimensionless flow rates in sections I and IV (m_I and m_{IV}), they were fixed with a safety margin from the point of minimum solvent consumption provided by the Triangle Theory, being 1.72 and 1.45, respectively. The simulation results are provided along with the studied system responses (extract purity, PuX; raffinate purity, PuR; and productivity, $Prod$) in Table 4 and the simulation grid is represented in Figure 8 by the black dots.

Table 4 – DoE grid runs for the optimization of the SMB separation of betulinic and oleanolic acids. Adsorbent: packing of Acclaim C30 column; mobile phase: methanol/acetonitrile 50/50 (%, v/v). $m_{\mathrm{I}} = 1.720$ and $m_{\mathrm{IV}} = 1.445$.

Factors		Responses		
m_{II}	m_{III}	PuX (%)	PuR (%)	$Prod$ (kg/($m^3_{adsorbent}$ day)
1.575	1.700	99.67	91.87	47.66
1.537	1.623	99.52	99.46	33.04
1.460	1.700	96.51	94.38	91.50
1.498	1.662	99.14	98.73	62.27
1.690	1.700	99.79	75.84	3.813
1.460	1.470	83.92	99.82	3.813
1.498	1.547	99.08	99.77	18.43
1.575	1.585	99.66	99.69	3.813
1.498	1.604	99.08	99.58	40.35
1.460	1.585	94.90	99.64	47.66
1.613	1.662	99.77	98.73	18.43
1.556	1.604	99.60	99.60	18.42
1.556	1.662	99.62	98.68	40.35

With the obtained responses for the considered grid points (factors), quadratic models were fitted to the simulation data of each purity response (PuX and PuR). For the productivity, a linear model was selected by default as productivity depends linearly on feed flow rate and, thus, on m_{II} and m_{III} [52]. The statistical significance of each term was carefully analyzed, and terms with p-value > 0.1 were deemed as insignificant and removed. The obtained reduced and uncodified models are given by:

$$PuX\ (\%) = -1304 + 16.98 m_{\mathrm{II}} + 1687 m_{\mathrm{III}} - 516 m_{\mathrm{III}}^2 \quad (12)$$

$$PuR\ (\%) = -1690 + 2374 m_{\mathrm{II}} - 777 m_{\mathrm{II}}^2 - 8.90 m_{\mathrm{III}}^2 \quad (13)$$

$$Prod\ (\mathrm{kg/(m^3_{adsorbent}\ day)}) = -381.2578 m_{\mathrm{II}} + 381.2513 m_{\mathrm{III}} \quad (14)$$

The obtained models presented coefficients of determination (R^2) and adjusted coefficients of determination (R^2_{adj}) of 0.895 and 0.859, 0.890 and 0.854, and 1.00 and 1.00, for the extract,

raffinate and productivity, respectively. These models were then applied to the multi-objective optimization of the betulinic and oleanolic acids separation to obtain the best operating conditions by imposing a minimum purity of 99 % in both extract and raffinate while simultaneously maximizing the productivity. The obtained results are listed in Table 5 and demonstrated that both acids can be obtained with purity of 99.2 % in both extract and raffinate with a productivity of 52.6 kg/($m^3_{adsorbent}$ day). Therefore, betulinic acid can be obtained in the raffinate stream at 2.61 g/day and the oleanolic acid at 3.27 g/day in the extract, considering 24 h operation under pseudo steady-state, both with 99.2 % purity. It is important to mention that the price *per* gram of each compound can easily reach four figures when purity increases above 99 % [67]. It is also worth of mention that the models slightly overestimated the minimum purity requirements, and thus underestimated the maximum productivity that would be obtained at 99 % extract and raffinate purity, but that was expectable since, as it was referred previously, the coefficients of determination (R^2) were 0.895 and 0.890 for the extract and raffinate, respectively. Additionally, the results compiled in Table 4 also demonstrated that higher purities of *ca.* 99.6 might be obtained for m_{II} and m_{III} values of 1.556 and 1.662, respectively, at the expense, of course, of a lower productivity. These results are illustrated in Figure 8 in which the separation region provided by the DoE-RSM approach as well as the optimum operation point are represented by the blue shaded area and red diamond symbol, respectively.

Comparing the results obtained in this work with methanol/acetonitrile 50/50 (%, v/v) and the packing material of the Acclaim C30 column with those achieved using the packing material of an Apollo C18 column with methanol/acetonitrile 50/50 (%, v/v) [30] and methanol/water 95/5 (%, v/v) [51], the productivity obtained here is at least 58.7 times superior, which clearly highlights that the proper selection of the stationary phase plays a crucial role in the SMB performance indicators. Particularly for the separation of betulinic and oleanolic acids, the Acclaim C30 column stationary phase provides remarkably good results.

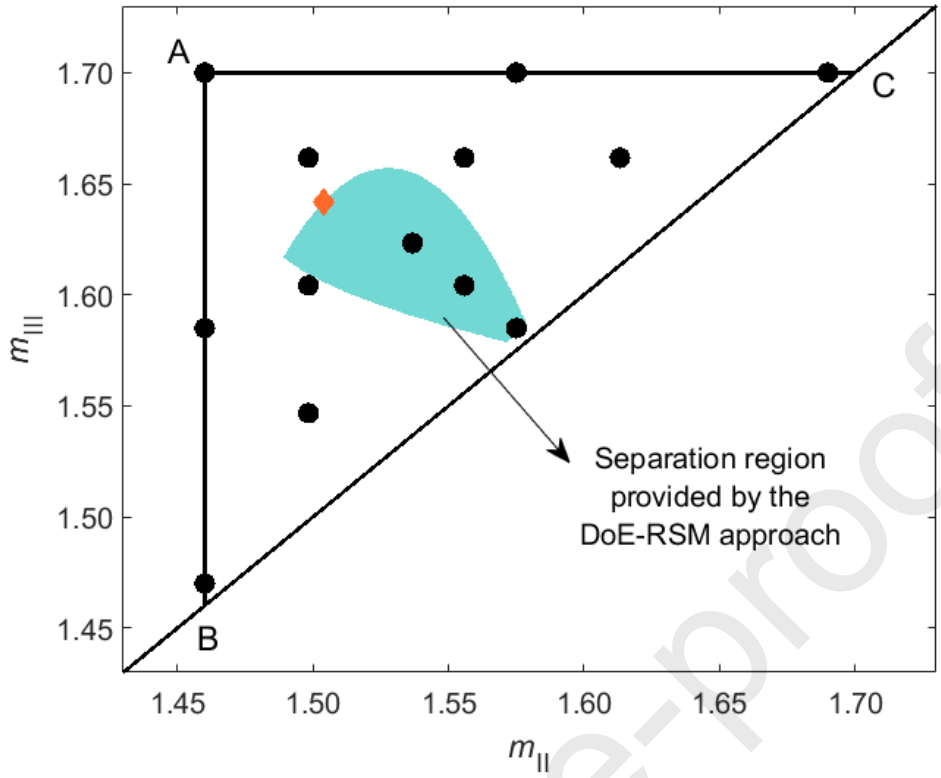

Figure 8 – Plane m_{II}-m_{III} showing: separation region provided by the Triangle theory ([ABCA]); DoE-RSM simulation grid (black dots); separation region provided by the DoE-RSM approach for which extract and raffinate are obtained with a minimum of 99 % purity (blue shaded area); and optimum separation point for a minimum of 99 % purity in extract and raffinate at maximum productivity (red diamond symbol).

Table 5 – Optimized operating conditions and simulation results for the separation of betulinic and oleanolic acids. Adsorbent: packing of Acclaim C30 column; mobile phase: methanol/acetonitrile 50/50 (%, v/v); temperature: 23 ºC.

Column configuration	1-1-1-1
m_{II}	1.504
m_{III}	1.642
t^* (min)	1.217
Q_{I} (mL/min)	34.31
Q_{II} (mL/min)	31.04
Q_{III} (mL/min)	33.13
Q_{IV} (mL/min)	30.16
Q_{E} (mL/min)	4.152
Q_{F} (mL/min)	2.083
Q_{X} (mL/min)	3.267
Q_R (mL/min)	2.968
$C_{\mathrm{BA}}^{\mathrm{X}}$(mg/mL)	0.005392
$C_{\mathrm{OA}}^{\mathrm{X}}$(mg/mL)	0.6956
$C_{\mathrm{BA}}^{\mathrm{R}}$(mg/mL)	0.6113
$C_{\mathrm{OA}}^{\mathrm{R}}$(mg/mL)	0.004677
PuX (%)	99.2
PuR (%)	99.2
$Prod$ (kg/($m^3_{adsorbent}$ day)	52.61
SC (m^3/kg)	1.50

E – eluent; F – feed; X – extract; R – raffinate; SC – solvent consumption

4.6. Water as TTAs recovery agent

The recovery of betulinic and oleanolic acids after their SMB separation is an equally important aspect to consider. It is known that the solubility of these ubiquitous pentacyclic triterpenoids in water or aqueous solutions is negligible when compared with organic solvents [34,68], and that the effect of water addition in their solubility is very pronounced, *i.e.*, small amounts of water

tend to induce sizeable reductions in their solubility [51,69–71]. Considering all this information, in this work the influence of water content in the solubility of betulinic and oleanolic acids in mixtures of methanol/acetonitrile/water was also addressed. According to the procedure presented in section 3.6, the solubility of pure betulinic and pure oleanolic acids was determined in 70/30, 50/50, and 30/70 (%, v/v) mixtures of methanol/acetonitrile modified with water from 0 % up to 65 % (v/v) at 23 °C. The obtained results are presented in Figure 9a – c. It is possible to see that, for both triterpenic acids, the solubilities decreased with the increase of water content as expected, but as the acetonitrile percentage is increased, distinct trends arose, *i.e.*, the solubility of oleanolic acid was not as severely affected with methanol/acetonitrile 30/70 (%, v/v) as it was with 50/50 and 70/30 (%, v/v) methanol/acetonitrile. For instance, while with methanol/acetonitrile 70/30 and 50/50 (%, v/v) the addition of 30 % (v/v) of water caused a solubility reduction of 95 % and 90 %, respectively, with methanol/acetonitrile 30/70 (% , v/v) a reduction of only 39 % occurred. For all mobile phases, a reduction in the solubility of at least 98 % is observed when 65 % (v/v) of water is added to all methanol/acetonitrile mixtures, allowing the recovery of triterpenic acids as pure precipitates.

After the precipitation of each TTA induced by water addition, it is necessary to remove such excessive water and refine the solvent mixture composition in order to recycle it to the SMB unit. At first glance, distillation can be adopted with success. However, mixtures of methanol/acetonitrile/water are difficult to fractionate as azeotropes between methanol/acetonitrile and acetonitrile/water exist. In the last few years extractive distillation, using glycerol as entrainer, has been regarded as a method to separate methanol/acetonitrile/water mixtures allowing the effective recovery of each solvent [72,73].

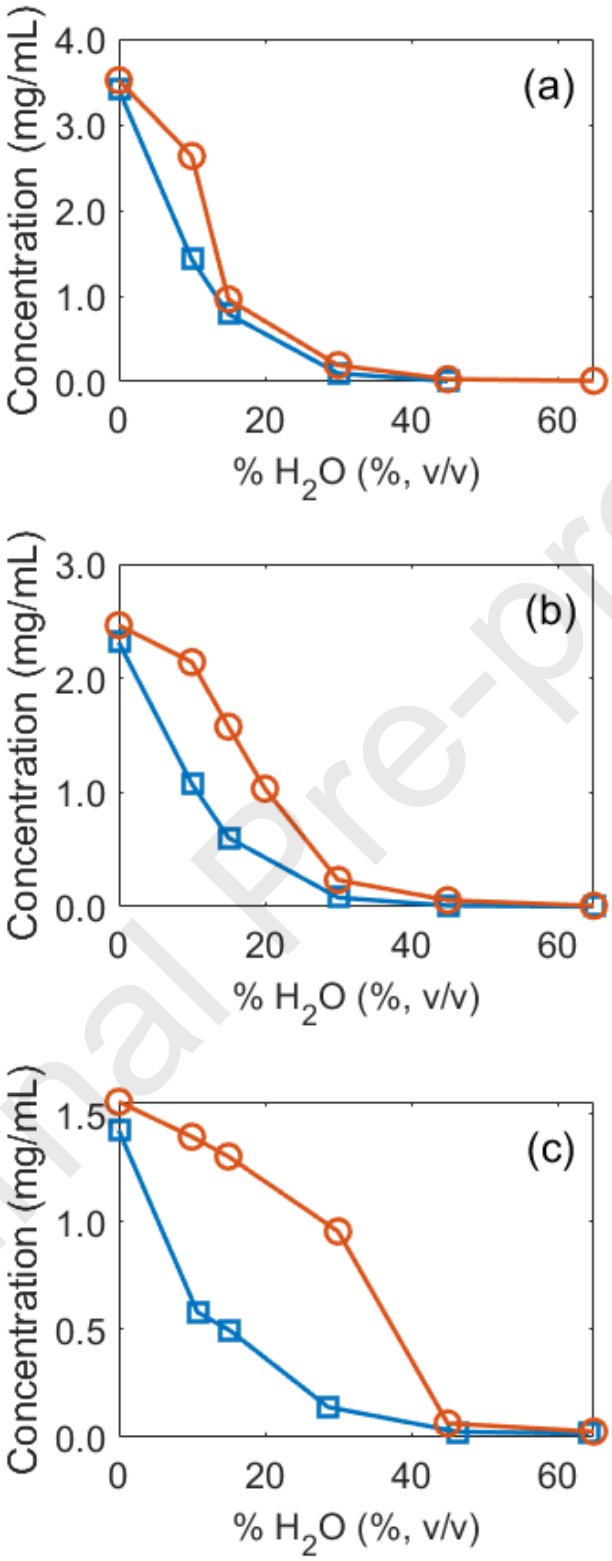

Figure 9 – Solubilities of pure betulinic (squares) and pure oleanolic (circles) acids at 23°C as function of water content in mobile phases of methanol/acetonitrile (a) 70/30 (%, v/v), (b) 50/50 (%, v/v), and (c) 70/30 (%, v/v).

5. Conclusions

The chromatographic separation of betulinic and oleanolic acids followed by a precipitation step was addressed in this work. Methanol, water, acetonitrile, ethanol, isopropanol, ethyl acetate, acetone and mixtures thereof were tested with an Acclaim C30 column (250 x 4.6, 5 µm), and the best mobile phase for the separation (in terms of compromise between selectivity and resolution and TTAs solubility) was methanol/acetonitrile 50/50 (%, v/v) at 23 ^{o}C.

The equilibrium and kinetic parameters of pure betulinic and pure oleanolic acids were obtained by the method of moments, and were successfully validated by modeling unary and binary breakthrough curves. Simulated moving bed calculations showed that both acids can be obtained with 99.2 % purity and productivity of 56.2 kg/($m^3_{adsorbent}$ day) using the packing material of an Acclaim C30 column with a 1-1-1-1 configuration with 7.5 cm columns. Finally, aiming for a TTA recovery solution, water was envisioned as a precipitation agent and the solubility of each TTA was measured in methanol/acetonitrile 70/30, 50/50, and 30/70 (%, v/v) modified with water. With the increase of acetonitrile content, the solubilities of oleanolic acids showed a weaker dependency on water content and the obtained results showed that a modification of at least 65 % (v/v) induces at least 98 % reduction in both TTAs solubilities in all the tested methanol/acetonitrile mixtures.

Acknowledgements

This work was developed within the scope of the project CICECO-Aveiro Institute of Materials, UIDB/50011/2020 & UIDP/50011/2020, financed by national funds through the Portuguese Foundation for Science and Technology/MCTES, and the Multibiorefinery project (POCI-01-0145-FEDER-016403). I.S. Azenha acknowledges a PhD grant from Fundação para Ciência e a

Tecnologia (Portugal) (grant number SFRH/BD/126509/2016) and financial support of Project POCI-01-0145-FEDER-006939 (Laboratory for Process Engineering, Environment, Biotechnology and Energy – LEPABE funded by FEDER funds through COMPETE2020 - Programa Operacional Competitividade e Internacionalização (POCI). The authors would also like to thank Mónica Válega (University of Aveiro) for the continuous support with the HPLC setup.

References

[1] J. Moncada B, V. Aristizábal M, C.A. Cardona A, Design strategies for sustainable biorefineries, Biochem. Eng. J. 116 (2016) 122–134. https://doi.org/10.1016/j.bej.2016.06.009.

[2] F. Cherubini, The biorefinery concept: Using biomass instead of oil for producing energy and chemicals, Energy Convers. Manag. 51 (2010) 1412–1421. https://doi.org/10.1016/J.ENCONMAN.2010.01.015.

[3] M. FitzPatrick, P. Champagne, M.F. Cunningham, R.A. Whitney, A biorefinery processing perspective: Treatment of lignocellulosic materials for the production of value-added products, Bioresour. Technol. 101 (2010) 8915–8922. https://doi.org/10.1016/j.biortech.2010.06.125.

[4] R.M.A. Domingues, A.R. Guerra, M. Duarte, C.S.R. Freire, C.P. Neto, C.M.S. Silva, A.J.D. Silvestre, Bioactive Triterpenic Acids: From Agroforestry Biomass Residues to Promising Therapeutic Tools, Mini. Rev. Org. Chem. 11 (2014) 382–399. https://doi.org/10.2174/1570193X113106660001.

[5] T. Ayeleso, M. Matumba, Oleanolic Acid and Its Derivatives: Biological Activities and Therapeutic Potential in Chronic Diseases, Molecules. 22 (2017) 1915. https://doi.org/10.3390/molecules22111915.

[6] J.L. Ríos, S. Máñez, New Pharmacological Opportunities for Betulinic Acid, Planta Med. 84 (2018) 8–19. https://doi.org/10.1055/s-0043-123472.

[7] C. Aiken, C.H. Chen, Betulinic acid derivatives as HIV-1 antivirals, Trends Mol. Med. 11 (2005) 31–36. https://doi.org/10.1016/j.molmed.2004.11.001.

[8] J. Pollier, A. Goossens, Oleanolic acid, Phytochemistry. 77 (2012) 10–15. https://doi.org/10.1016/j.phytochem.2011.12.022.

[9] S. Jäger, H. Trojan, T. Kopp, M. Laszczyk, A. Scheffler, S. Jäger, H. Trojan, T. Kopp, M.N. Laszczyk, A. Scheffler, Pentacyclic Triterpene Distribution in Various Plants – Rich Sources for a New Group of Multi-Potent Plant Extracts, Molecules. 14 (2009) 2016–2031. https://doi.org/10.3390/molecules14062016.

[10] M.K. Shanmugam, X. Dai, A.P. Kumar, B.K.H. Tan, G. Sethi, A. Bishayee, Oleanolic acid and its synthetic derivatives for the prevention and therapy of cancer: Preclinical and clinical evidence, Cancer Lett. 346 (2014) 206–216. https://doi.org/10.1016/j.canlet.2014.01.016.

[11] M.E. Juan, J.M. Planas, Effects of Pentacyclic Triterpenes from Olives on Colon Cancer, in: Bioact. Foods Extr. Cancer Treat. Prev., CRC Press, 2010: pp. 403–413.

[12] J.L.C. Sousa, C.S.R. Freire, A.J.D. Silvestre, A.M.S. Silva, Recent Developments in the Functionalization of Betulinic Acid and Its Natural Analogues: A Route to New Bioactive Compounds, Molecules. 24 (2019) 355. https://doi.org/10.3390/molecules24020355.

[13] C. Xu, B. Wang, Y. Pu, J. Tao, T. Zhang, Techniques for the analysis of pentacyclic triterpenoids in medicinal plants, J. Sep. Sci. 41 (2018) 6–19. https://doi.org/10.1002/jssc.201700201.

[14] J.P.S. Aniceto, C.M. Silva, Preparative Chromatography: Batch and Continuous, in: Anal. Sep. Sci., Wiley-VCH Verlag GmbH & Co. KGaA, Weinheim, Germany, 2015: pp. 1207–

1313. https://doi.org/10.1002/9783527678129.assep047.

[15] S. Guo, J.A. Duan, Y.P. Tang, N.Y. Yang, D.W. Qian, S.L. Su, E.X. Shang, Characterization of triterpenic acids in fruits of *Ziziphus* species by HPLC-ELSD-MS, J. Agric. Food Chem. 58 (2010) 6285–6289. https://doi.org/10.1021/jf101022p.

[16] C. Bérangère, N. Caussarieu, P. Morin, L. Morin-Allory, M. Lafosse, Rapid analysis of triterpenic acids by liquid chromatography using porous graphitic carbon and evaporative light scattering detection, J. Sep. Sci. 27 (2004) 964–970. https://doi.org/10.1002/jssc.200401764.

[17] L. Olmo-García, A. Bajoub, A. Fernández-Gutiérrez, A. Carrasco-Pancorbo, Evaluating the potential of LC coupled to three alternative detection systems (ESI-IT, APCI-TOF and DAD) for the targeted determination of triterpenic acids and dialcohols in olive tissues, Talanta. 150 (2016) 355–366. https://doi.org/10.1016/j.talanta.2015.12.042.

[18] D.I. Falev, D.S. Kosyakov, N. V. Ul'yanovskii, D. V. Ovchinnikov, Rapid simultaneous determination of pentacyclic triterpenoids by mixed-mode liquid chromatography–tandem mass spectrometry, J. Chromatogr. A. 1609 (2020) 460458. https://doi.org/10.1016/j.chroma.2019.460458.

[19] G.L. Li, J.M. You, C.H. Song, L. Xia, J. Zheng, Y.R. Suo, Development of a new HPLC method with precolumn fluorescent derivatization for rapid, selective and sensitive detection of triterpenic acids in fruits, J. Agric. Food Chem. 59 (2011) 2972–2979. https://doi.org/10.1021/jf104224t.

[20] S. Zhang, Y. Sun, Z. Sun, X. Wang, J. You, Y. Suo, Determination of triterpenic acids in fruits by a novel high performance liquid chromatography method with high sensitivity and specificity, Food Chem. 146 (2014) 264–269. https://doi.org/10.1016/j.foodchem.2013.09.056.

[21] Z. Zheng, X.E. Zhao, S. Zhu, J. Dang, X. Qiao, Z. Qiu, Y. Tao, Simultaneous Determination of Oleanolic Acid and Ursolic Acid by in Vivo Microdialysis via UHPLC-MS/MS Using Magnetic Dispersive Solid Phase Extraction Coupling with Microwave-Assisted Derivatization and Its Application to a Pharmacokinetic Study of Arcti, J. Agric. Food Chem. 66 (2018) 3975–3982. https://doi.org/10.1021/acs.jafc.7b06015.

[22] Z. Zeng, W. Zhou, N. Hu, L. Zou, B. Bai, H. Wang, Comparison of using two different labeling reagents for rapid analysis of triterpenic acids by pre-column derivatization with RP-HPLC-FLD and application to plant samples, Anal. Methods. 11 (2019) 4354–4361. https://doi.org/10.1039/c9ay01357a.

[23] E. Giménez, M.E. Juan, S. Calvo-Melià, J. Barbosa, V. Sanz-Nebot, J.M. Planas, Pentacyclic triterpene in *Olea europaea* L: A simultaneous determination by high-performance liquid chromatography coupled to mass spectrometry, J. Chromatogr. A. 1410 (2015) 68–75. https://doi.org/10.1016/j.chroma.2015.07.064.

[24] E. Giménez, M.E. Juan, S. Calvo-Melià, J.M. Planas, A sensitive liquid chromatography-mass spectrometry method for the simultaneous determination in plasma of pentacyclic triterpenes of *Olea europaea* L., Food Chem. 229 (2017) 534–541. https://doi.org/10.1016/j.foodchem.2017.02.116.

[25] M. Tarvainen, J.-P. Suomela, H. Kallio, B. Yang, Triterpene Acids in *Plantago major*: Identification, Quantification and Comparison of Different Extraction Methods, Chromatographia. 71 (2010) 279–284. https://doi.org/10.1365/s10337-009-1439-7.

[26] M. Strzemski, M. Wójciak-Kosior, I. Sowa, E. Rutkowska, W. Szwerc, R. Kocjan, M. Latalski, *Carlina* species as a new source of bioactive pentacyclic triterpenes, Ind. Crops Prod. 94 (2016) 498–504. https://doi.org/10.1016/j.indcrop.2016.09.025.

[27] P. Srivastava, R. Chaturvedi, Simultaneous determination and quantification of three

pentacyclic triterpenoids-betulinic acid, oleanolic acid, and ursolic acid-in cell cultures of *Lantana camara* L., Vitr. Cell. Dev. Biol. - Plant. 46 (2010) 549–557. https://doi.org/10.1007/s11627-010-9298-3.

[28] S. Wang, H. Zhao, J. Jiang, G. Liu, C. Yang, Analysis of three types of triterpenoids in tetraploid white birches (*Betula platyphylla* Suk.) and selection of plus trees, J. For. Res. 26 (2015) 623–633. https://doi.org/10.1007/s11676-015-0096-y.

[29] C.M. Andre, L. Larsen, E.J. Burgess, D.J. Jensen, J.M. Cooney, D. Evers, J. Zhang, N.B. Perry, W.A. Laing, Unusual immuno-modulatory triterpene-caffeates in the skins of russeted varieties of apples and pears, J. Agric. Food Chem. 61 (2013) 2773–2779. https://doi.org/10.1021/jf305190e.

[30] I.S. Azenha, J.P.S. Aniceto, S.P. Sequeira, A. Mendes, C.M. Silva, Chromatographic separation of betulinic and oleanolic acids, Sep. Purif. Technol. 235 (2020) 116129. https://doi.org/10.1016/j.seppur.2019.116129.

[31] S.H. Nile, A. Nile, J. Liu, D.H. Kim, G. Kai, Exploitation of apple pomace towards extraction of triterpenic acids, antioxidant potential, cytotoxic effects, and inhibition of clinically important enzymes, Food Chem. Toxicol. 131 (2019) 110563. https://doi.org/10.1016/j.fct.2019.110563.

[32] Y. Sun, F. Feng, B. Nie, J. Cao, F. Zhang, High throughput identification of pentacyclic triterpenes in *Hippophae rhamnoides* using multiple neutral loss markers scanning combined with substructure recognition (MNLSR), Talanta. 205 (2019) 120011. https://doi.org/10.1016/j.talanta.2019.06.011.

[33] L. Stebounova, S.M. Ebert, L.T. Murry, C.M. Adams, D.J. Murry, Rapid and Sensitive Quantification of Ursolic Acid and Oleanolic Acid in Human Plasma Using Ultra-performance Liquid Chromatography-Mass Spectrometry, J. Chromatogr. Sci. 56 (2018)

644–649. https://doi.org/10.1093/chromsci/bmy038.

[34] S. Jäger, K. Winkler, U. Pfüller, A. Scheffler, Solubility studies of oleanolic acid and betulinic acid in aqueous solutions and plant extracts of *Viscum album* L., Planta Med. 73 (2007) 157–162. https://doi.org/10.1055/s-2007-967106.

[35] L. Pereira, Porous Graphitic Carbon as a Stationary Phase in HPLC: Theory and Applications, J. Liq. Chromatogr. Relat. Technol. 31 (2008) 1687–1731. https://doi.org/10.1080/10826070802126429.

[36] B. Rhourri-Frih, P. Chaimbault, D. Dequeral, P. André, M. Lafosse, Investigation of porous graphitic carbon for triterpenoids and natural resinous materials analysis by high performance liquid chromatography hyphenated to mass spectrometry, J. Chromatogr. A. 1240 (2012) 140–146. https://doi.org/10.1016/j.chroma.2012.03.094.

[37] C.G. Grigoras, E. Destandau, L. Fougère, C. Elfakir, Evaluation of apple pomace extracts as a source of bioactive compounds, Ind. Crops Prod. 49 (2013) 794–804. https://doi.org/10.1016/j.indcrop.2013.06.026.

[38] T.E. Bapiro, F.M. Richards, D.I. Jodrell, Understanding the Complexity of Porous Graphitic Carbon (PGC) Chromatography: Modulation of Mobile-Stationary Phase Interactions Overcomes Loss of Retention and Reduces Variability, Anal. Chem. 88 (2016) 6190–6194. https://doi.org/10.1021/acs.analchem.6b01167.

[39] K. Zhang, X. Liu, Mixed-mode chromatography in pharmaceutical and biopharmaceutical applications, J. Pharm. Biomed. Anal. 128 (2016) 73–88. https://doi.org/10.1016/j.jpba.2016.05.007.

[40] Y. Yang, X. Geng, Mixed-mode chromatography and its applications to biopolymers, J. Chromatogr. A. 1218 (2011) 8813–8825. https://doi.org/10.1016/j.chroma.2011.10.009.

[41] L.C. Sander, S.A. Wise, Effect of phase length on column selectivity for the separation of

polycyclic aromatic hydrocarbons by reversed-phase liquid chromatography, Anal. Chem. 59 (1987) 2309–2313. https://doi.org/10.1021/ac00145a020.

[42] K. Makino, H. Ozaki, H. Imaishi, T. Takeuchi, T. Fukui, A RPLC C 30 Column for the Separation of Oligonucleotides, Chem. Lett. 16 (1987) 1251–1254. https://doi.org/10.1246/cl.1987.1251.

[43] L.C. Sander, K.E. Sharpless, N.E. Craft, S.A. Wise, Development of Engineered Stationary Phases for the Separation of Carotenoid Isomers, Anal. Chem. 66 (1994) 1667–1674. https://doi.org/10.1021/ac00082a012.

[44] K. Albert, Correlation between chromatographic and physicochemical properties of stationary phases in HPLC: C30 bonded reversed-phase silica, TrAC Trends Anal. Chem. 17 (1998) 648–658. https://doi.org/10.1016/S0165-9936(98)00074-0.

[45] L.C. Sander, K.E. Sharpless, M. Pursch, C30 Stationary phases for the analysis of food by liquid chromatography, J. Chromatogr. A. 880 (2000) 189–202. https://doi.org/10.1016/S0021-9673(00)00121-7.

[46] C.A. Rimmer, L.C. Sander, S.A. Wise, Selectivity of long chain stationary phases in reversed phase liquid chromatography, Anal. Bioanal. Chem. 382 (2005) 698–707. https://doi.org/10.1007/s00216-004-2858-9.

[47] L.C. Sander, C.A. Rimmer, W.B. Wilson, Characterization of triacontyl (C-30) liquid chromatographic columns, J. Chromatogr. A. 1614 (2019) 460732. https://doi.org/10.1016/j.chroma.2019.460732.

[48] M. Plante, B. Bailey, C. Crafts, I.N. Acworth, Sensitive HPLC Method for Triterpenoid Analysis Using Charged Aerosol Detection with Improved Resolution, 2016.

[49] J.P.S. Aniceto, S.P. Cardoso, C.M. Silva, General optimization strategy of simulated moving bed units through design of experiments and response surface methodologies,

Comput. Chem. Eng. 90 (2016) 161–170. https://doi.org/10.1016/j.compchemeng.2016.04.028.

[50] D.M. Ruthven, Principles of Adsorption and Adsorption Processes, John Wiley & Sons, New York, 1984.

[51] J.P.S. Aniceto, I.S. Azenha, F.M.J. Domingues, A. Mendes, C.M. Silva, Design and optimization of a simulated moving bed unit for the separation of betulinic, oleanolic and ursolic acids mixtures: Experimental and modeling studies, Sep. Purif. Technol. 192 (2018) 401–411. https://doi.org/https://doi.org/10.1016/j.seppur.2017.10.016.

[52] A. Rajendran, G. Paredes, M. Mazzotti, Simulated moving bed chromatography for the separation of enantiomers, J. Chromatogr. A. 1216 (2009) 709–738. https://doi.org/10.1016/j.chroma.2008.10.075.

[53] K. Miyabe, Moment theory for kinetic study of chromatography, TrAC - Trends Anal. Chem. 81 (2016) 79–86. https://doi.org/10.1016/j.trac.2016.01.003.

[54] M. Li, Z. Bao, H. Xing, Q. Yang, Y. Yang, Q. Ren, Simulated moving bed chromatography for the separation of ethyl esters of eicosapentaenoic acid and docosahexaenoic acid under nonlinear conditions, J. Chromatogr. A. 1425 (2015) 189–197. https://doi.org/10.1016/j.chroma.2015.11.041.

[55] X. Wang, C.B. Ching, Determination of the Competitive Adsorption Isotherms of Nadolol Enantiomers by an Improved h-Root Method, in: Ind. Eng. Chem. Res., American Chemical Society , 2003: pp. 6171–6180. https://doi.org/10.1021/ie0303698.

[56] M.F. Edwards, J.F. Richardson, Gas dispersion in packed beds, Chem. Eng. Sci. 23 (1968) 109–123. https://doi.org/10.1016/0009-2509(68)87056-3.

[57] A. Veseli, S. Žakelj, A. Kristl, A review of methods for solubility determination in biopharmaceutical drug characterization, Drug Dev. Ind. Pharm. 45 (2019) 1717–1724.

https://doi.org/10.1080/03639045.2019.1665062.

[58] S.P.L. Sequeira, Separação de compostos bioativos para a indústria farmacêutica por leito móvel simulado, Universidade de Aveiro, 2017.

[59] W. Long, Easy Method Transfer and Improved Performance with Agilent InfinityLab Poroshell 120 4 µm Columns, 2017. https://www.agilent.com/cs/library/applications/5991-5510EN.pdf (accessed February 26, 2020).

[60] Grace Davison Discovery Sciences, Grace HPLC Column Families, 2011. https://www.hplc.eu/Downloads/GRACE_HPLC_Column_Families.pdf (accessed February 27, 2020).

[61] Agilent Technologies, LC AND LC/MS - Your Essential Resource for Columns & Supplies, 2012. https://www.agilent.com/cs/library/catalogs/public/5991-1059EN LC_Columns.pdf (accessed February 27, 2020).

[62] Thermo Fisher Scientific Inc., Connected chromatography solutions - 2019/2021 Chromatography Consumables Catalog, 2019. https://assets.thermofisher.com/TFS-Assets/CMD/Catalogs/BR-21443-Chromatography-Catalog-LC-BR21443-EN.pdf (accessed February 27, 2020).

[63] M.M.R. de Melo, E.L.G. Oliveira, A.J.D. Silvestre, C.M. Silva, Supercritical fluid extraction of triterpenic acids from *Eucalyptus globulus* bark, J. Supercrit. Fluids. 70 (2012) 137–145. https://doi.org/10.1016/j.supflu.2012.06.017.

[64] R.M.A. Domingues, M.M.R. de Melo, E.L.G. Oliveira, C.P. Neto, A.J.D. Silvestre, C.M. Silva, Optimization of the supercritical fluid extraction of triterpenic acids from *Eucalyptus globulus* bark using experimental design, 74 (2013) 105–114. https://doi.org/10.1016/j.supflu.2012.12.005.

[65] Thermo Fisher Scientific Inc., Acclaim C30 Columns - Product Manual, 2018.

[66] I.S. Azenha, J.P.S. Aniceto, C.A. Santos, A. Mendes, C.M. Silva, Enhanced separation of bioactive triterpenic acids with a triacontylsilyl silica gel adsorbent: From impulse and breakthrough experiments to the design of a simulated moving bed unit, Sep. Purif. Technol. 248 (2020) 116991. https://doi.org/10.1016/j.seppur.2020.116991.

[67] Sigma-Aldrich, (n.d.). https://www.sigmaaldrich.com/ (accessed April 16, 2020).

[68] L. Liu, X. Wang, Solubility of oleanolic acid in various solvents from (288.3 to 328.3) K, J. Chem. Eng. Data. 52 (2007) 2527–2528. https://doi.org/10.1021/je700312r.

[69] I.J. Jin, Y.I. Ko, Y.M. Kim, S.K. Han, Solubilization of oleanolic acid and ursolic acid by cosolvency, Arch. Pharm. Res. 20 (1997) 269–274. https://doi.org/10.1007/BF02976156.

[70] J.P. Fan, T. Kong, X.H. Zhang, L. Zhang, S. Tong, Z.Y. Tian, J.H. Zhu, Solubilities of oleanolic acid and ursolic acid in (ethanol + water) mixed solvents from T = (292.2 to 328.2) K, J. Chem. Thermodyn. 47 (2012) 372–375. https://doi.org/10.1016/j.jct.2011.11.017.

[71] J.P. Fan, Y.H. Cao, X.H. Zhang, D.Q. Jiang, J.X. Yu, Determination and Modeling of the Solubilities of Oleanolic Acid and Ursolic Acid in Ethanol + Sodium Hydroxide + Water Mixed Solvents from T = 283.2 to 323.2 K, J. Chem. Eng. Data. 62 (2017) 3991–3997. https://doi.org/10.1021/acs.jced.7b00686.

[72] V.M. Raeva, A.Y. Sazonova, Separation of ternary mixtures by extractive distillation with 1,2-ethandiol and glycerol, Chem. Eng. Res. Des. 99 (2015) 125–131. https://doi.org/10.1016/j.cherd.2015.04.032.

[73] Y. Wang, G. Bu, X. Geng, Z. Zhu, P. Cui, Z. Liao, Design optimization and operating pressure effects in the separation of acetonitrile/methanol/water mixture by ternary extractive distillation, J. Clean. Prod. 218 (2019) 212–224. https://doi.org/10.1016/j.jclepro.2019.01.324.

Author Statement

Ivo S. Azenha: Writing - original draft; Investigation; Methodology

José P.S. Aniceto: Writing - original draft; Methodology; Formal analysis

Diogo P. Ribeiro: Investigation; Methodology

Adélio Mendes: Supervision; Writing - review & editing; Formal analysis;

Carlos M. Silva: Funding acquisition; Supervision; Writing - review & editing; Conceptualization; Resources; Formal analysis

Highlights

Reversed phase HPLC separation of betulinic and oleanolic acids with C30 column

Multiple solvents and mixtures thereof studied for their chromatographic separation

Method of moments used to quickly determine equilibrium and mass transfer parameters

SMB optimization and acids isolation with purities of 99 % in a 1-1-1-1 SMB unit

Downstream recovery of betulinic and oleanolic acids by precipitation using water